

PARTS-BASED SHAPE RECOGNITION VIA SHAPE GEODESICS

Mayss'aa Merhy^{1,2}, Abdesslam Benzinou¹, Kamal Nasreddine¹, Mohamad Khalil², Ghaleb Faour³¹UEB, Ecole Nationale d'Ingénieurs de Brest (ENIB), UMR CNRS 6285 Lab-STICC, 29238 BREST cedex, France²Azm Platform for Research in Biotechnology and Its Applications, Lebanese University, Tripoli, Lebanon³National Council for Scientific Research (CNRS), P.O. Box: 11-8281, Beirut, Lebanon

ABSTRACT

The quality of the segmentation process directly affects the performance of the shape recognition. In this paper, we address the problem of shape recognition using only the available shape parts instead of the whole shape. For this purpose, we propose a shape parts recognition strategy that uses a robust distance based on geodesics in the shape space. The proposed combining strategy seeks to handle the contour discontinuity that can occur in edge maps due to various disturbing factors encountered in real images. The experimental validation through the *MPEG-7* shape database and some real images demonstrates the efficiency of our proposed approach.

Index Terms— shape recognition, shape parts, combining strategy, geodesics, real images

1. INTRODUCTION

The quality of the segmentation process directly affects the performance of the subsequent processing steps in high-level tasks as shape recognition. Despite considerable research and progress in this field [1], a complete segmentation into continuous contours cannot be achieved in all cases and remains a challenging problem. Discontinuities in contours can be caused by several factors such as distortion, illumination variation, noise, segmentation errors or overlap and occlusion of objects in digital images. Due to these various factors, it is often unreachable to segment the entire object and only some contour parts/fragments of objects can be detected as illustrated in Fig.1. To tackle this problem, some recent works propose edge grouping to seek salient contours [2-5]. Generally, the edge grouping methods aim to identify a subset of contour fragments and group them into complete boundaries [2, 3] or into meaningful contour parts [4, 5] by combining some well-known Gestalt laws such as the closure, the proximity, the continuity and the convexity. Numerous are the edge grouping methods but existing algorithms are extremely unstable. Furthermore, they do not provide a general solution to all kinds of discontinuity sources that can occur in natural images.

Far from the concept of using edge grouping algorithms to group shape contour parts, we propose a novel method for shape recognition based on the available
















Input image	Edge map	Retained contourparts	Assigned class
			→ Butterfly
			→ Cattle
			→ Horseshoe
			→ Hammer
			→ Guitar

Fig.1. Examples of real images (in the first column) and the corresponding contour maps (in the second column). In the third column, we show pairs of shape contour parts issued from segmented images marked by blue and red. The fourth column gives the image class assigned by our approach.

shape parts. The present paper is an extension of our work presented in [6, 7] where we performed shape recognition when we have the whole shape (i.e. closed curve). Our objective here is to develop a new framework for shape recognition using a novel strategy of combining contour parts information. We aim to explore the improvement resulting from using the relationship existing between shape parts in the shape recognition domain. The originality of this work is twofold. On one hand, we propose an elastic shape similarity measure based on shape geodesics for shape parts comparison. On the other hand, we propose a parts-based strategy aiming to reach a more accurate decision in shape recognition using multiple parts of the object shape issued from the segmentation process.

Generally, it is difficult to recognize a shape by knowing only one part of its contour. In [8], it is shown that the recognition process obviously depends on the selected part that must be significant and representative of its original shape. This one-shape-part based shape recognition system often leads to a non-guaranteed successful recognition. A novel formulation of chamfer matching and a class-specific codebook of contour fragments have been proposed as a powerful combination for object detection and object recognition [9]. Based on

Thanks to AUF for funding.

the fact that all contour fragments contain both local and global shape information, the approach in [10, 11] adopted contour fragments as key shape features for learning a shape codebook. A new shape representation called bag of contour fragments (BCF) inspired by classical bag of words (BoW) is recently developed in [10]. The same authors applied in [11] a new shape descriptor named vector of aggregated contour fragments (VACF) to shape classification task. In [12], a new study focuses on the frequent contour segments (FCSs) for describing shape contour using frequently appearing patterns; a genetic algorithm is used to search for the fragments that are repeated and similar. So, it is clearly remarkable that most of the state-of-the-art methods for shape parts based shape recognition assume having all shape contour parts information of a given shape. However, this is not often found on realistic situations.

This paper is organized as follows. Section 2 provides a description of our proposed shape recognition system. In this section, we present our geodesics-based distance, we describe the building of the labeled shape parts database, and we give the proposed parts-based strategy. Section 3 is devoted to validate the proposed shape recognition system through the *MPEG-7* dataset. In addition, we present experiments carried out on real images given in Fig. 1. Concluding remarks are reported in section 4.

2. PARTS-BASED SHAPE RECOGNITION SYSTEM

Parts-based shape recognition is the process of recognizing shapes by analyzing the information issued from shape parts comparison. In this section, we propose a novel parts-based shape recognition scheme that exploits a robust metric based on shape geodesics. The proposed parts-based strategy combines parts recognition outputs for the recognition of the whole shape.

2.1. Geodesics-based distance

Geodesics in shape space correspond to optimal deformations that align one curve to another as described in [6, 7]. The core of our work relies on the definition of a similarity measure between two open planar curves. Let Q and P be two significant shape parts, we firstly establish a robust registration between the two given shape parts parameterized as two 1D signals. Wherefore, we search for the optimal mapping function ϕ^* that maps the curvilinear abscissa on the first segment Q to its corresponding curvilinear abscissa on the second segment P using the following formulation:

$$\phi^* = \underset{\phi}{\operatorname{argmin}} \left(\arccos \int_0^1 \sqrt{\phi_s(s)} \left| \cos \frac{\|\theta_Q(s) - \theta_P(\phi(s))\|_\rho}{2} \right| ds \right), \quad (1)$$

where the open curves Q and P are represented by their tangent functions θ_Q and θ_P respectively. Note that these functions are parameterized by the arclength s after having normalized each open curve to the length one. The robust Leclerc estimator $\|\cdot\|_\rho$ is used to penalize possible

aberrant values. The term $\sqrt{\phi_s(s)}$ penalizes the torsion and stretching along the curves and $\phi_s(s) = \frac{d\phi(s)}{ds}$.

Once the optimal mapping function ϕ^* is obtained, our geodesics based distance D_{partial} is defined as the robust registration residual error established between the two contour parts Q and P as:

$$D_{\text{partial}}(Q, P) = \arccos \int_0^1 \sqrt{\phi_s^*(s)} \left| \cos \left(\frac{\theta_Q(s) - \theta_P(\phi^*(s))}{2} \right) \right| ds, \quad (2)$$

The proposed similarity measure should be invariant under scaling, translation and rotation of shape outlines. The scale factor and the translation impacts are removed when we use the angle function parameterized by the normalized curvilinear abscissa as signature. However, different methods are proposed to solve the orientation problem. Often in the quadratic distance based approaches [13, 14], the orientation invariance is achieved by finding the optimal shifting angle. In [15] a Procruste alignment algorithm is used for this purpose. Here, we choose to use the invariant segment representation method proposed in [16] as a rotation invariant scheme for shape parts due to the fact that an optimization algorithm is a time consuming method.

2.2. Building of labeled shape parts database

As there is no database of shape parts, we propose to build a database of labeled shape parts starting from a database of complete shapes. We assume that the original database includes n_C classes, $(C_k)_{k=1, \dots, n_C}$; each class consists of n_I different instances, $(I_j)_{j=1, \dots, n_I}$. We denote by (I_j, C_k) an instance I_j that belongs to the class C_k . Here, we decompose each instance to n_P significant shape parts; n_P depends on the instance to be fragmented. According to this scheme, we then obtain a set of labeled contour parts $\{P_i^{j,k}\}_{i=1, \dots, n_P}$ where $P_i^{j,k}$ denotes the i^{th} shape part of the instance (I_j, C_k) . Each part is represented by N sampling points.

The database construction scheme should effectively extract the shape contour fragments so that they are suitable for parts-based shape recognition. Firstly, the outline of each given shape is simplified into a meaningful polygon via the Discrete Curve Evolution method (DCE) [11]. For example, the closed contour of the *Deer* in Fig. 2 (a) is represented by the simplified polygon illustrated in Fig. 2 (b). Then, we use the vertices of the simplified polygon to obtain the main visual parts of its corresponding original contour. A shape part is defined as a fragment from the original contour limited by non-consecutive pair of the obtained vertices. In the second row in Fig. 2, we show some extracted contour parts relying on the common vertices, of the simplified polygon (b) and the original contour (a), marked with black circles in Fig. 2 (c). Finally, we exclude from our database all the contour parts with relatively small x and y variances (< 0.11) in their invariant representation. Following these steps, we construct a database of labeled contour parts having relevant shape information.

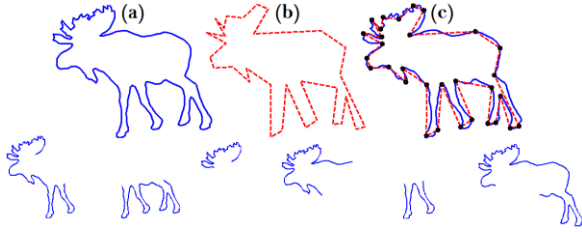


Fig. 2. (a): the contour of a *Deer* shape. (b): the DCE simplified polygon of (a). (c): common vertices of polygon (b) on the original contour (a) marked as black circles. The second row illustrates some contour parts.

2.3. Parts-based recognition strategy

We assume having from a segmented image a number n_Q of parts of the shape to recognize, so we have a set of queries $\{Q_r\}_{r=1,\dots,n_Q}$. Initially, each query is compared separately to the labeled shape parts. Then, we combine parts recognition outputs in order to recognize the entire shape. The proposed parts-based recognition strategy involves the following six steps:

- Step 1: For each query Q_r , look for the set S_r of the K most similar shape parts according to the geodesics based distance, D_{partial} , calculated at a low sampling level l where shape parts are represented by M_l points ($M_l < N$).
- Step 2: Determine, for each query Q_r , the set C_r of the classes to which belong the elements of S_r :

$$C_r = \{C_k / \exists P_i^{j,k} \in S_r\}.$$
- Step 3: Find the common set C of candidate classes as

$$C = C_1 \cap C_2 \cap \dots \cap C_{n_Q}.$$
- Step 4: Compare each query Q_r to the shape parts subset, $\{P_i^{j,k} / C_k \in C\}$, at the superior original sampling level with N points.
- Step 5: For each instance (I_j, C_k) under the constraint that $C_k \in C$, compute the global distance D from the set of queries $\{Q_r\}$ as:

$$D(\{Q_r\}, (I_j, C_k)) = \sum_{r=1}^{n_Q} \min_{1 \leq i \leq n_P} D_{\text{partial}}(Q_r, P_i^{j,k}), \quad (3)$$
- Step 6: the recognition of the input shape is then performed with the obtained global distance D .

3. PERFORMANCE EVALUATION

In order to validate experimentally the proposed parts-based shape recognition, we use the part B of the MPEG-7 shape database. This database is composed of a large number of real and synthetic shapes: 70 classes of shapes with 20 examples of each class. For the learning database, we construct a database of labeled shape parts by using shapes 1-10 in each of the 70 classes of the MPEG-7 dataset. Following the database building method described in section 2.2, we obtain a database of nearly 60,000 labeled shape parts (i.e. $|\{P_{i,j,k}\}| = 60,000$). For evaluation purposes, we firstly use five shapes from shapes 11-20 in some classes. We extract two shape parts from each used shape to be studied as queries. Selected pairs of queries (Q_1, Q_2) of each shape are given in the

first line of table 1 by blue contour part (with circle extremities) and by red one (with cross extremities) respectively. We investigate by this experiment the case when the shape is occluded and the total segmentation of the shape is not possible.

Elephant,C.34	Camel,C.10	Horse,C.48	Apple,C.1	Cattle,C.13
R_1 : 50% R_2 : 40%	R_1 : 40% R_2 : 60%	R_1 : 40% R_2 : 30%	R_1 : 60% R_2 : 40%	R_1 : 20% R_2 : 0%
R : 100%	R : 80%	R : 100%	R : 100%	R : 100%
C.34, 0.3855	C.10, 0.5095	C.48, 0.3928	C.1, 0.2270	C.13, 0.2764
C.34, 0.4797	C.10, 0.5312	C.48, 0.5206	C.1, 0.3089	C.13, 0.4491
C.34, 0.4969	C.10, 0.5638	C.48, 0.5549	C.1, 0.3191	C.13, 0.4692
C.34, 0.5331	C.10, 0.5870	C.48, 0.5684	C.1, 0.3778	C.13, 0.4842
C.34, 0.5514	C.10, 0.6234	C.48, 0.6230	C.1, 0.3985	C.13, 0.5464
C.34, 0.5687	C.10, 0.6456	C.48, 0.7022	C.1, 0.4050	C.13, 0.5866
C.34, 0.6019	C.10, 0.6568	C.48, 0.7188	C.1, 0.4381	C.13, 0.5896
C.34, 0.6049	C.15, 0.6633	C.48, 0.7402	C.1, 0.5207	C.13, 0.6096
C.34, 0.6429	C.15, 0.6831	C.48, 0.7557	C.1, 0.5225	C.13, 0.6425
C.34, 0.6457	C.10, 0.6849	C.48, 0.7650	C.1, 0.5599	C.13, 0.6551

Table 1. Retrieval results using our method on MPEG-7 queries. 1st row: the retained contour parts as queries for the 5 test instances. 3rd row: retrieval rates R_1 and R_2 for Q_1 and Q_2 respectively. 4th row: retrieval rate R for combined queries. In the retaining rows, we show the corresponding 10 retrieved shapes. (C.x, D): x is the class number in MPEG-7 and D is the global distance to the query (Eq. 3).

For the step 1 of our algorithm described in the section 2.3, the adopted low sampling level is of 50 points (i.e. $M_l = \frac{N}{2} = 50$). For each pair of queries (Q_1, Q_2) , the

retrieval rates R_1 and R_2 (row 3 of table 1) are measured as the percentage of shape parts that belong to the same class of Q_1 and Q_2 respectively among the 10 most similar parts. We can observe that some queries have retrieval rates better than others. For example, the queries Q_2 of the *Camel* instance and Q_1 of the *Apple* instance lead both to 60% of correct retrieval rate because they are significant parts that characterize original shapes. But

combination is based here on the 20 most similar shape parts to each query ($K = 20$). Then we compare each pair of queries to the instances of the common set of the candidate classes \mathcal{C} ($N = 100$ points). We count the number of instances coming from the same class among the first 10 most similar shapes (showed below each query). For each pair of queries, the retrieval rate R (row 4) outperforms the retrieval rates R_1 and R_2 when each




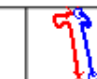
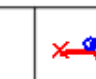



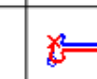



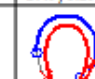

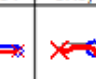
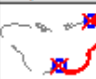







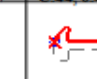
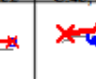













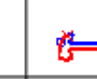
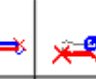

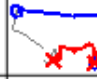

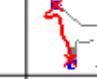
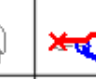



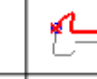
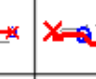
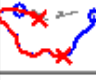
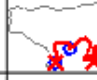

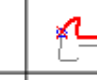
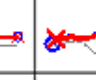
				
Butterfly, C.9	Cattle, C.13	Horseshoe, C.49	Hammer, C.44	Guitar, C.43
R_1 : 10% R_2 : 30%	R_1 : 0% R_2 : 50%	R_1 : 60% R_2 : 80%	R_1 : 80% R_2 : 100%	R_1 : 50% R_2 : 100%
R : 100%	R : 70%	R : 100%	R : 90%	R : 100%
				
C.9, 0.5484	C.48, 0.4883	C.49, 0.2914	C.44, 0.4534	C.43, 0.4472
				
C.9, 0.5567	C.48, 0.5400	C.49, 0.3138	C.44, 0.4534	C.43, 0.4482
				
C.9, 0.5662	C.13, 0.5582	C.49, 0.3197	C.44, 0.4652	C.43, 0.4642
				
C.9, 0.5721	C.13, 0.5629	C.49, 0.3246	C.44, 0.4652	C.43, 0.4728
				
C.9, 0.5818	C.48, 0.5706	C.49, 0.3369	C.44, 0.4652	C.43, 0.4867
				
C.9, 0.6425	C.13, 0.5829	C.49, 0.3440	C.44, 0.4652	C.43, 0.4966
				
C.9, 0.6444	C.13, 0.5837	C.49, 0.3502	C.44, 0.4743	C.43, 0.5059
				
C.9, 0.7320	C.13, 0.5913	C.49, 0.3840	C.44, 0.5102	C.43, 0.5070
				
C.9, 0.7348	C.13, 0.5923	C.49, 0.3902	C.44, 0.5302	C.43, 0.5178
				
C.9, 0.7476	C.13, 0.5936	C.49, 0.4163	C.44, 0.5311	C.43, 0.5798

Table 2. Retrieval results using our method on real images. 1st row: the retained contour parts from real images of Fig. 1. The remaining rows have the same organization as in table 1.

when the query is not representative, it will not be unique and there will be a lot of parts similar to it. For example, the query Q_2 of the *Cattle* instance is not significant (retrieval rate of 0%). In order to improve retrieval success rates, we apply our combining strategy. The




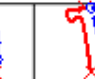


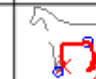

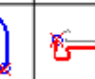
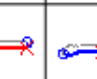

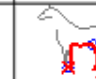

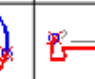
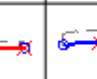

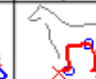


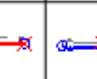






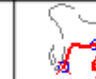


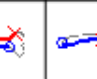

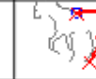



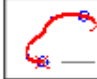


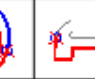











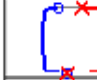
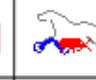

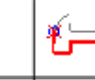

				
Butterfly, C.9	Cattle, C.13	Horseshoe, C.49	Hammer, C.44	Guitar, C.43
R_1 : 0% R_2 : 0%	R_1 : 0% R_2 : 40%	R_1 : 20% R_2 : 90%	R_1 : 30% R_2 : 80%	R_1 : 50% R_2 : 100%
R : 0%	R : 0%	R : 100%	R : 70%	R : 100%
				
C.45, 0.4097	C.48, 0.2846	C.49, 0.1485	C.44, 0.2353	C.43, 0.2007
				
C.26, 0.4643	C.48, 0.2957	C.49, 0.1538	C.44, 0.2538	C.43, 0.2139
				
C.45, 0.4708	C.48, 0.3059	C.49, 0.1605	C.44, 0.2538	C.43, 0.2304
				
C.45, 0.4857	C.48, 0.3130	C.49, 0.1650	C.6, 0.2796	C.43, 0.2319
				
C.45, 0.4871	C.48, 0.3308	C.49, 0.1666	C.6, 0.2796	C.43, 0.2463
				
C.26, 0.4900	C.48, 0.3422	C.49, 0.1802	C.6, 0.2987	C.43, 0.2482
				
C.45, 0.4925	C.48, 0.4029	C.49, 0.1816	C.44, 0.3013	C.43, 0.2576
				
C.45, 0.5055	C.48, 0.4512	C.49, 0.1884	C.44, 0.3013	C.43, 0.2618
				
C.26, 0.5098	C.48, 0.4641	C.49, 0.2531	C.44, 0.3013	C.43, 0.2838
				
C.26, 0.5167	C.48, 0.4847	C.49, 0.2607	C.44, 0.3013	C.43, 0.3237

Table 3. Retrieval results using the SC-based approach on real images. 1st row: the retained contour parts from real images of Fig. 1. The remaining rows have the same organization as in table 1.

query is investigated alone. It reaches at minimum 80% of correct retrieval (*Camel* queries) and it rises to 100% for the other queries. Hence, the obtained results validate the

proposed parts-based recognition strategy as an efficient shape recognition system.

To generalize our geodesics based recognition approach, we evaluate its performance on some real images. For this goal, we use the five images illustrated in the first column of Fig.1. From the edge map, we take the two most significant contour parts as queries (third column of Fig.1). Our experimental retrieval results performed on these real images are illustrated in table 2. It is remarkable that in the most of the cases the retrieval rate of the combined queries outperforms the retrieval rate of each query considered alone. For the purposes of comparative evaluations, we implemented the shape context (SC) based approach presented in [8]. Shape contexts are distributions represented as Log-polar histograms. Even if the shape context is the most adopted descriptor in the literature for shape part comparison, it has a main drawback which resides on a messy correspondence of points. Using the SC-based distance, we apply the proposed shape recognition strategy on the same images. The experimental results are shown in table 3. The shape context based approach definitely fails to retrieve correctly the *Butterfly* and the *Cattle* queries ($R = 0\%$), while our geodesics based method does not. Hence, we can infer the high efficiency of our geodesics based method for handling elastic deformation.

Regarding to the shape parts correspondence issue, the geodesics based approach performs correct parts correspondence in the most of the cases. Correct recognition can be also accompanied with incorrect correspondences between parts when the studied shape encloses symmetric aspect as the cases of the *Butterfly* (column 1 of table 2) and the *Guitar* (column 5 of table 2). We can also clearly see that in the case where our geodesics based approach fails to recognize a given pair of queries, it maps to the queries some shape parts visually similar while the shape context method does not. For example, both methods retrieve *Horse* instances as the two most similar shapes to *Cattle* queries (rows 1 and 2 of the tables 1 and 2). However, the shape parts of the retrieved horses by the geodesics method are visually more similar to the queries. On the other hand, the shape parts of the horses mapped to the queries by the shape context method are not so relevant.

Finally, the proposed geodesics based method is also exploited for shape classification on the same pairs previously used for shape retrieval (in tables 2 and 3). With the *10-Nearest-Neighbors* classification, we assign to each pair (as query) the majority class among the 10 most similar. Our method yields always to a correct classification, while the other method assigns false classes to the *Butterfly* and the *Cattle* queries. Hence, our method also performs better than the shape context method for shape classification.

3. CONCLUSION

In this paper we propose a new shape recognition scheme. We integrate here a geodesics based distance for shape parts comparison and a parts-based recognition strategy.

Our experimental results demonstrate the outperformance of the proposed approach compared to the shape context approach for shape parts correspondence and for shape recognition.

REFERENCES

- [1] N. Senthilkumaran, R. Rajesh, "Edge detection techniques for image segmentation—a survey of soft computing approaches", *International Journal of Recent Trends in Engineering and Technology (IJRTET)*, vol. 1, no 2, 2009.
- [2] C. Lu, L. J. Latecki, N. Adluru, X. Yang, H. Ling, "Shape guided contour grouping with particle filters", *IEEE 12th International Conference on Computer Vision (ICCV)*, pp.2288-2295, 2009.
- [3] Y. Qi, J. Guo, Y. Li, H. Zhang, T. Xiang, Y. Song, "Sketching by perceptual grouping", *IEEE Conference on Image Processing (ICIP)*, 2013.
- [4] L. J. Latecki, R. Lakaemper, "Polygonal approximation of laser range data based on perceptual grouping and EM", *IEEE Conference in Robotics and Automation (ICRA)*, pp. 790-796, 2006.
- [5] J. S. Stahl, K. Oliver, S. Wang, "Open boundary capable edge grouping with feature maps", *IEEE Conference on Computer Vision and Pattern Recognition Workshop (CVPRW)*, pp.1-8, 2008.
- [6] K. Nasreddine, A. Benzinou and R. Fablet, "Variational shape matching for shape classification and retrieval", *Pattern Recognition Letters*, vol. 31, no 12, pp. 1650-1657, 2010.
- [7] M. Merhy, A. Benzinou, K. Nasreddine, M. Khalil and G. Faour, "An optimal elastic partial shape matching via shape geodesics", *IEEE Conference on Image Processing (ICIP)*, France, 2014.
- [8] X. Bai, X. Yang, L. J. Latecki, "Detection and recognition of contour parts based on shape similarity", *Pattern Recognition*, vol. 41, no 7, pp. 2189-2199, 2008.
- [9] J. Shotton, A. Blake, R. Cipolla, "Multiscale categorical object recognition using contour fragments", *IEEE Transactions on Pattern Analysis and Machine Intelligence*, vol. 30, no 7, pp. 1270-1281, 2008.
- [10] X. Wang, B. Feng, X. Bai, W. Liu, L. J. Latecki, "Bag of contour fragments for robust shape classification", *Pattern Recognition*, vol. 47, no 6, pp. 2116-2125, 2014.
- [11] S. Bai, X. Wang, X. Bai, "Aggregating contour fragments for shape classification", *IEEE Conference on Image Processing (ICIP)*, France, 2014.
- [12] H. Wei, X. S. Tang, "A genetic-algorithm-based explicit description of object contour and its ability to facilitate recognition", *IEEE Transactions on Cybernetics*, 2014.
- [13] L. J. Latecki, R. Lakamper, D. Wolter, "Optimal partial shape similarity", *Image and Vision Computing*, vol. 23, no 2, pp. 227-236, 2005.
- [14] M. Tanase, R. C. Veltkamp, "Part-based shape retrieval", *13th Annual Conference on Multimedia (ACM)*, Singapore, pp. 543-546, 2005.
- [15] G. McNeil, S. Vijayakumar, "Hierarchical Procrustes Matching for shape retrieval", *IEEE Conference on Computer Vision and Pattern Recognition (CVPR)*, USA, pp. 885-894, 2006.
- [16] K. B. Sun, B. J. Super, "Classification of contour shapes using class segment sets", *IEEE Conference on Computer Vision and Pattern Recognition (CVPR)*, USA, pp. 727-733, 2005.